Anesthesiology 2010; 113:1406–18

Identification of the Epidural Space with Optical Spectroscopy

An In Vivo *Swine Study*

James P. Rathmell, M.D.,* Adrien E. Desjardins, Ph.D.,† Marjolein van der Voort, Ph.D.,† Benno H. W. Hendriks, Ph.D.,§ Rami Nachabe, M.Sc.,‖ Stefan Roggeveen, Ir.,# Drazenko Babic, M.D.,** Michael Söderman, M.D., Ph.D.,†† Marcus Brynolf, M.D.,‡‡ Björn Holmström, M.D., Ph.D.§§

ABSTRACT

Background: Accurate identification of the epidural space is critical for safe and effective epidural anesthesia or treatment of acute lumbar radicular pain with epidural steroid injections. The loss-of-resistance technique is commonly used, but it is known to be unreliable. Even when it is performed in conjunction with two-dimensional fluoroscopic guidance, determining when the needle tip enters the epidural space can be challenging. In this swine study, we investigated whether the epidural space can be identified with optical spectroscopy, using a custom needle with optical fibers integrated into the cannula.

Methods: Insertion of the needle tip into the epidural space was performed with midline and paramedian approaches in a swine. In each insertion, optical spectra were acquired at different insertion depths, and anatomical localization of the needle was determined by three-dimensional imaging with rotational C-arm computed tomography. Optical spectra that included both visible and near-infrared wavelength ranges were processed to derive estimates of the blood and lipid volume fractions.

Results: In all insertions, the transition of the needle tip to the epidural space from an adjacent tissue structure (interspinous ligament or the ligamentum flavum) was found to be associated with an increase in the lipid volume fraction. These increases, which ranged from 1.6- to 3.0-fold, were statistically significant ($P = 0.0020$). Lipid fractions obtained from the epidural space were 1.9- to 20-fold higher than those obtained from muscle ($P = 0.0013$). Accidental penetration of an epidural vein during one insertion coincided with a high blood volume fraction.

Conclusions: The spectroscopic information obtained with the optical spinal needle is complementary to fluoroscopic images, and it could potentially allow for reliable identification of the epidural space during needle placement.

What We Already Know about This Topic.

- ❖ Identification of the epidural space during needle insertion relies on feel, which can be misleading.

What This Article Tells Us That Is New

- ❖ In one anesthetized pig, optical spectra at the epidural needle tip displayed a large increase in lipid volume fraction upon entering the epidural space.
- ❖ Optical imaging may provide direct, nontactile feedback of epidural space entry with a needle.

EPIDURAL injection is a common intervention for providing surgical anesthesia as well as for treating acute radicular pain associated with lumbar intervertebral disc herniation.[1] Accurately identifying the epidural space during these procedures can be challenging. The loss-of-resistance (LOR) technique is most frequently used for identification, but in the absence of confirmatory methods, it is often inaccurate. It has been estimated that the LOR technique is inaccurate in up to 53% of cervical epidural steroid injections

* Associate Professor of Anaesthesia, Department of Anesthesia, Critical Care and Pain Medicine, Massachusetts General Hospital/Harvard Medical School, Boston, Massachusetts, † Senior Scientist, § Research Fellow, ‖ Research Assistant, # Venture Manager, Philips Research, Eindhoven, The Netherlands, ** Clinical Scientist, Philips Healthcare, Best, The Netherlands, †† Associate Professor, Department of Clinical Neuroscience, Karolinska Institutet, Stockholm, Sweden, and Department of Neuroradiology, Karolinska University Hospital, Solna, Stockholm, Sweden, ‡‡ Resident, Department of Anesthesiology and Intensive Care, Karolinska University Hospital, Huddinge, Stockholm, Sweden, §§ Department of Clinical Science, Intervention and Technology, Karolinska Institutet, and Department of Anesthesiology and Intensive Care, Karolinska University Hospital, Huddinge, Sweden.

Received from the Department of Clinical Science, Intervention and Technology, Karolinska Institutet, Stockholm, Sweden. Submitted for publication May 7, 2010. Accepted for publication September 7, 2010. Support provided by Philips Research, Eindhoven, The Netherlands.

Address correspondence to Dr. Holmström: Department of Anesthesiology and Intensive Care, B31, Karolinska University Hospital, Huddinge, SE-141 86 Stockholm, Sweden. bjorn.holmstrom@karolinska.se.

when used without image guidance.[2] Failure of the LOR can occur when dense ligamentum flavum is absent, so that significant resistance to injection is not encountered.[3]

Complications associated with epidural injections have been well documented.[1] The most frequent complication is placement of the injected solution in a location outside of the epidural space, which is likely to result in inadequate anesthesia for surgical procedures (epidural anesthesia) and to reduce the efficacy of treatment for radicular pain (epidural steroid injections). Dural puncture can result in postdural puncture headache and placement of solutions within the cerebrospinal fluid, resulting in spinal rather than epidural anesthesia; the safety of the excipient containing the steroid in this context is uncertain.[4] Intravascular injections of local anesthetic or particulate steroids, which can occur even when aspiration is negative for blood,[5] can result in cardiorespiratory arrest, central nervous system toxicity, and ischemic neurologic events in the spinal cord and brain.[1] Spinal cord damage[6] and paralysis after injection within the spinal cord[7] have also been reported.

Fluoroscopic guidance has resulted in significant improvements in the accuracy of needle tip localization and has reduced complication rates; as such, it is strongly recommended for patients receiving epidural steroid injections.[8] A recent study found that intrathecal needle placement still occurred in 0.5% of interlaminar lumbar epidural steroid injection procedures in which both fluoroscopy and the LOR technique were used.[9] Fluoroscopic guidance remains impractical for routine use in surgical and obstetric anesthesia.

Recently, optical identification of the epidural space with a porcine model was demonstrated.[10] In that study, a custom stylet with integrated optical fibers, positioned in a Tuohy needle, was used to deliver and receive light at two different wavelengths in the visible range. Although the results are very promising, several important questions remained unaddressed. First, how do optical signals acquired from the needle correspond to physiologic parameters of tissue? Second, can adipose tissue present in the epidural space be identified using measurements in the near-infrared range, where optical contrast for lipids is particularly high and not confounded by the presence of hemoglobin? Third, can optical signals be used to identify intravascular and intrathecal needle placement? The present study, designed and conducted without knowledge of the study of Ting *et al.*,[10] addresses these questions. A custom optical spinal needle designed for practical use during regional anesthesia was used. It has optical fibers embedded in the cannula that allow for optical spectroscopic measurements to be acquired from tissues close to the bevel surface of the needle tip. We performed insertions to the epidural space of a swine *in vivo*, with both midline and paramedian approaches. During each insertion, we obtained optical spectra spanning visible and near-infrared wavelengths at multiple insertion depths. Differences in optical spectra associated with the corresponding tissue transitions were quantified with a spectral processing algorithm that derived estimates of the blood and lipid volume fractions in tissues close to the bevel surface of the needle tip.

Materials and Methods

Anesthesia and Monitoring

Experiments were performed at Karolinska University Hospital with Internal Review Board approval (Northern Regional Ethics Committee for Animal Research, Stockholm, Sweden). Given general anesthesia, a Swedish Landrace swine (42 kg; male) was positioned on a fluoroscopy table in the left lateral decubitus position. General anesthesia was induced with sodium thiopental and maintained with sodium thiopental and fentanyl infusions throughout the experiment. Mechanical ventilation and continuous monitoring of heart rate and pulse oximetry were performed.

Optical Spinal Needle

The design of the optical spinal needle was derived from an 18-gauge spinal injection needle with a Quincke model tip. Three optical fibers (core diameter: 200 μm) were embedded in the needle shaft, so that they terminated at the bevel surface. One fiber was located near the distal end of the bevel surface and delivered broadband light, which was scattered and absorbed by the tissue in front of the needle tip. The two other optical fibers were located at the proximal end of the bevel surface, at a distance of 2.4 mm from the distal fiber; they received light scattered within tissue and directed it to two spectrometers where it was spectrally resolved across the wavelength range of 500–1,600 nm. From each spectrum that was acquired from tissue, a background spectrum that was acquired with the broadband light shuttered was subtracted to compensate for ambient light and detector dark currents. The intensities of the background-subtracted spectra were calibrated relative to a spectrum that was acquired from a white reflectance standard before all of the insertions. For each location of the needle tip, the optical spinal needle provided a spectrum that derived from tissue located approximately 1.2 mm or closer to the bevel surface. Spectra were acquired with an integration time of 0.5 s.

Image Guidance

Image guidance was provided with a 20-cm flat detector angiography system (Allura Xper FD20; Philips Healthcare, Best, The Netherlands), which allowed for both two-dimensional fluoroscopic imaging and three-dimensional rotational C-arm computed tomography (XperCT).[11] XperCT imaging was based on a motorized circular movement of the C-arm with a motion range of 240°, during which 620 rotational fluoroscopic frames were acquired. Reconstruction and visualization were performed with a three-dimensional rotational angiography workstation.

Before each insertion, the needle trajectory was planned in software with the three-dimensional rotational angiography workstation following XperCT imaging.[12] This software uses XperCT images to calculate the angle of insertion and distance required to advance a needle along a direct path from the skin entry point to the desired target, which in this study was the epidural space. At the location on the skin

identified by the planning software, an introducer needle was first inserted superficially such that the tip reached a depth of approximately 5 mm relative to the skin surface. It was subsequently removed, and the optical spinal needle was inserted along this predetermined path. Previous placement of the rigid introducer needle facilitated insertion of the more flexible optical spinal needle through the thick swine skin.

Image-guided Insertions

Numerous image-guided needle insertions to the epidural space were performed. The needle trajectory from the skin's surface to the epidural space was altered to simulate various needle paths that are common during localization of the epidural space, including midline insertion, lateral deviation superficial to the epidural space, and a paramedian approach. Insertions were carried out at lumbar and thoracic levels. During one insertion, the needle entered an epidural vein on entry into the epidural space, allowing measurement of the spectral characteristics of this common problematic needle position. During each insertion, the needle was advanced through anteriorly beyond the epidural space to allow measurement of the spectral characteristics of entry into the cerebrospinal fluid (CSF), spinal cord, and the intervertebral disc. We note that the conus medullaris of the spinal cord typically extends to the sacral level in swine.[13]

During each insertion, the optical spinal needle was advanced in discrete increments aimed at placing the needle at specific anatomic levels (*e.g.*, in the muscle superficial to the interspinous ligament, within the interspinous ligament, and within the epidural space). The needle was held in precise position at each depth using a custom-built radiolucent clamp. Anteroposterior and lateral fluoroscopic guidance was used to judge the approximate needle depth at each level, and the precise anatomic position was then determined using XperCT images. At each needle position, 20 optical spectra were acquired in addition to an XperCT image. Positioning of the needle within the epidural space was based on the XperCT images and was performed without use of the loss-of-resistance method to avoid the introduction of air or saline into the epidural space, which would distort the optical spectra. During the image-guided insertions, spectra were not displayed to the practitioner performing the insertions to assure that the identification of the epidural space was determined anatomically using the XperCT images and was not affected by the spectroscopic information.

Optically Guided Insertions

After the image-guided insertions, five insertions were performed in which guidance to the epidural space target was performed solely with the interpretation of optical spectra. These optically guided insertions were performed at consecutive lumbar levels with midline and paramedian approaches. During the insertions, spectra were acquired continuously, with a tissue spectrum and a corresponding background spectrum acquired approximately once every second; they were displayed to an independent member of the research team who interpreted them in real time without knowledge of the needle position. Interpretation was performed by visually comparing spectra displayed during the procedure with spectra acquired during the image-guided insertions. Specifically, the interpreter sought to identify a prominent lipid absorption peak centered at 1,210 nm that was similar to those observed in spectra previously acquired from the epidural space with x-ray guidance. After the identification of this peak, the needle was fixed in position, and an XperCT image was acquired to determine the anatomic position of the needle tip. Spectral analysis, as described in the following section, was not performed in real time and was not available to the interpreter during this pilot study. The practitioner who performed the optically guided needle insertions was blinded to the optical spectra and did not have x-ray image guidance; the only feedback provided during a given insertion occurred at the end, with an alert from the interpreter indicating that the prominent lipid absorption peak had been identified.

Spectral Analysis

To obtain quantitative estimates of chromophore volume fractions from diffuse reflectance spectra, a computational model of light propagation was used. The model accepted chromophore volume fractions and light-scattering parameters as input and generated a spectrum as output. Estimates were revised iteratively to minimize the difference between the spectrum generated by the model and acquired from tissue. This method of spectral analysis was first developed to analyze spectra acquired from colon polyps[14] and was recently modified to include absorption by lipids in a study by Nachabé *et al.*[15] It was assumed that the tissue regions from which the spectra was derived were optically homogeneous. The light propagation model was applied separately to the spectra obtained from the two spectrometers. For spectra in the range of 500–1,000 nm, the dominant chromophores were assumed to be oxyhemoglobin and deoxyhemoglobin. For spectra in the range of 900–1,600 nm, the dominant chromophores were assumed to be water and lipid. With the aforementioned iteration method, two parameters were estimated: the blood fraction and the lipid fraction. The former parameter is defined as the estimated total concentration of hemoglobin (the sum of the concentrations of oxyhemoglobin and deoxyhemoglobin) and is expressed as a percentage of the total concentration of hemoglobin in normal human blood (150 g/liter). The latter parameter is defined as the estimated volume fraction of lipid normalized by the sum of the estimated volume fractions of lipid and water. Analysis of each spectrum took 4.5 s, with processing performed in MATLAB (Mathworks, Natick, MA) on a 2.4-GHz laptop computer.

Statistical Analysis

Two statistical analyses were performed to determine the significance of the changes in blood and lipid fractions obtained from image-guided insertions. The first analysis fo-

cused on changes in the parameters corresponding to transitions in individual needle insertions. For each pair of adjacent tissues, a two-tailed *t* test for paired samples (unequal variances) was applied to compare the parameters obtained with the needle tip at one location with those obtained with the needle tip at the second location. To examine the repeatability of using the optical guidance technique, a second analysis was carried out by combining the blood and lipid fraction values from all five needle insertions. Two-tailed *t* tests for paired samples (unequal variances) were applied to compare the mean blood and lipid fractions obtained with the needle tip (1) in muscle *versus* in the epidural space and (2) at ligamentous tissues just superficial to the epidural space (interspinous ligament or the ligamentum flavum) *versus* in the epidural space. With all analyses, those yielding a P value <0.05 were considered significant. Bonferroni corrections were applied to adjust for multiple comparisons; the level of significance for each analysis was set as follows: insertions 1 and 3, 4 comparisons, $P < 0.0125$ (0.05/4) was considered significant; insertions 2 and 5, 3 comparisons, $P < 0.0167$ (0.05/3) was considered significant; insertion 4, 2 comparisons, $P < 0.025$ (0.05/2) was considered significant.

Results

Image-guided Insertions

Sagittal and axial cross-sections extracted from the XperCT images provided excellent visualization of the needle, the spine, and the soft tissues, including the spinal cord and posterior skeletal muscles, allowing precise anatomic localization of the needle tip. During needle insertion in the midline at the lumbar level (fig. 1A), sagittal and axial XperCT images show the position of the needle tip at five different depths. The epidural space—the adipose-rich region surrounding the spinal cord—could clearly be identified within the vertebral column as a thin region of lower x-ray attenuation relative to the CSF-containing thecal sac. The needle boundaries were slightly blurred because of x-ray attenuation discontinuities; at the distal part of the needle, these artifacts were slightly more pronounced. With surface reconstructions of the XperCT image volumes, the needle trajectory and the spinal geometry were clearly visualized, as shown for the first midline insertion in figure 1B.

The corresponding optical spectra obtained at each needle position are displayed as the intensity of light received from tissue as a function of the wavelength of light (fig. 1A). Optical spectra varied as the needle tip was positioned in different tissues. These variations could be characterized in terms of absorption peaks, which manifested as lower intensities within specific wavelength ranges. There was good correspondence between the spectral locations of the observed absorption peaks and those of known chromophores. It is likely that absorption peaks present between 500 and 600 nm derived in large part from hemoglobin.[16] The predominance of deoxygenated or oxygenated forms could be inferred from the shape of the spectra between 500 and 600 nm, with the former having a single absorption peak at 557 nm and the latter with two at 542 and 576 nm. An additional small absorption peak centered at 757 nm was probably associated with the presence of the deoxygenated forms. The presence of lipid is probably responsible for absorption peaks centered at 930 nm and 1,210 nm,[17,18] with the latter more pronounced; the presence of water is responsible for absorption peaks observed at 976, 1,197, and 1,455 nm.[19] The blood and lipid fractions are shown together with the corresponding optical spectra in figure 1A; these same parameters are concatenated in figure 1C to show their variation as the needle tip progressed ventrally, demonstrating their potential for tissue differentiation.

Figure 1 illustrates a midline approach to the lumbar epidural space. The transition of the needle tip from skeletal muscle to the epidural space was associated with a large increase in the lipid fraction (mean ± SD: 5.3 ± 0.4% to 47.6 ± 0.4%) and a decrease in the blood fraction (2.06 ± 0.01% to 0.183 ± 0.002%). With the needle tip in the interspinous ligament, intermediate values were observed for the two parameters (23.30 ± 0.09% and 0.769 ± 0.006%, respectively). As the needle tip progressed beyond the epidural space through the intrathecal space and into the intervertebral disc, little change in the blood fraction was observed; the lipid fraction decreased to 1.9 ± 0.1%. Figure 2 illustrates entry into a vein within the epidural space. The transition of the needle tip from skeletal muscle to the epidural space was associated with an increase in the lipid fraction (19.1 ± 0.6% to 53.2 ± 0.2%), which was similar in magnitude to that observed in the first midline insertion. With the needle tip at the interspinous ligament, an intermediate lipid fraction was observed again (28.7 ± 0.3%). With the needle tip in the epidural space, the mean blood fraction was more than 7-fold higher than those at the previous two locations and 27-fold higher than it was in the first midline insertion. When the stylet was removed with the cannula in place, spontaneous backflow of venous blood consistent with the puncture of an epidural vein was observed. With the needle tip in the intrathecal space, the mean blood fraction was higher than in the first midline insertion, and the mean lipid fraction was lower; removal of the stylet revealed backflow of blood-tinged CSF.

Figure 3 illustrates deviation of the needle tip from the interspinous ligament to the lumbar paravertebral skeletal muscle, superficial to the epidural space and then through the lateral portion of the ligamentum flavum and into the epidural space. The transition from interspinous ligament to the paravertebral muscle was associated with a decrease in the lipid fraction (57.4 ± 0.3% to 38.2 ± 0.8%) and an increase in the blood fraction (0.596 ± 0.006% to 1.26 ± 0.01%). Likewise, with the first two insertions, transition of the needle tip from skeletal muscle to the epidural space resulted in a higher lipid fraction (74 ± 1%) and a lower mean blood fraction (0.241 ± 0.006%). With the needle tip at the ligamentum flavum, intermediate values were observed for the

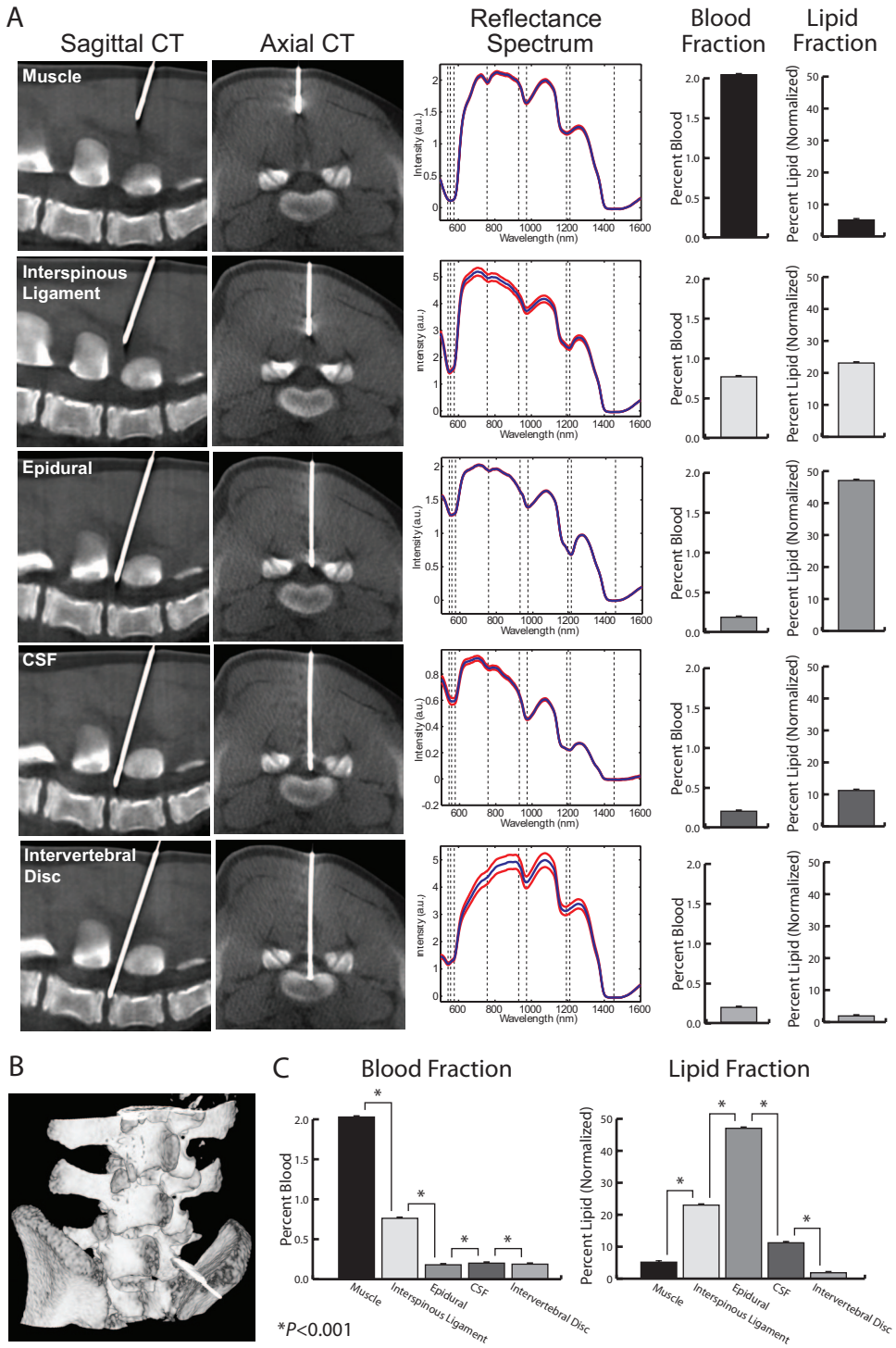

Fig. 1. Lumbar interlaminar midline approach to the epidural space (L5/6). (*A*) Sagittal and axial cross-sections extracted from the XperCT image volumes (*left*) for five needle tip locations: muscle, interspinous ligament, epidural space, cerebrospinal fluid (CSF), and intervertebral disc. The corresponding optical spectra and the blood and lipid fractions are shown on the *right*. The optical spectra indicate the intensity of light received by the optical spinal needle (linear units) as a function of the wavelength. Mean spectral values (*blue*) and SD relative to the mean (*red*) are displayed as a function of wavelength. Specific wavelengths corresponding to selected absorption peaks are indicated with *dashed lines*. Oxyhemoglobin: 542 and 576 nm; deoxyhemoglobin: 557 and 757 nm; lipids: 930 and 1,210 nm; water: 976, 1197, 1,455 nm. (*B*) Surface rendering of the XperCT volume indicating the needle trajectory relative to the spine. (*C*) Blood and lipid fractions concatenated to indicate their variation as the needle tip progressed ventrally. An *asterisk* indicates a transition for which the corresponding parameter change within this insertion was statistically significant at the level of $P < 0.001$ using two-tailed *t* tests for paired samples ($P < 0.0125$ considered significant after Bonferroni correction for multiple comparisons). CT = computed tomography.

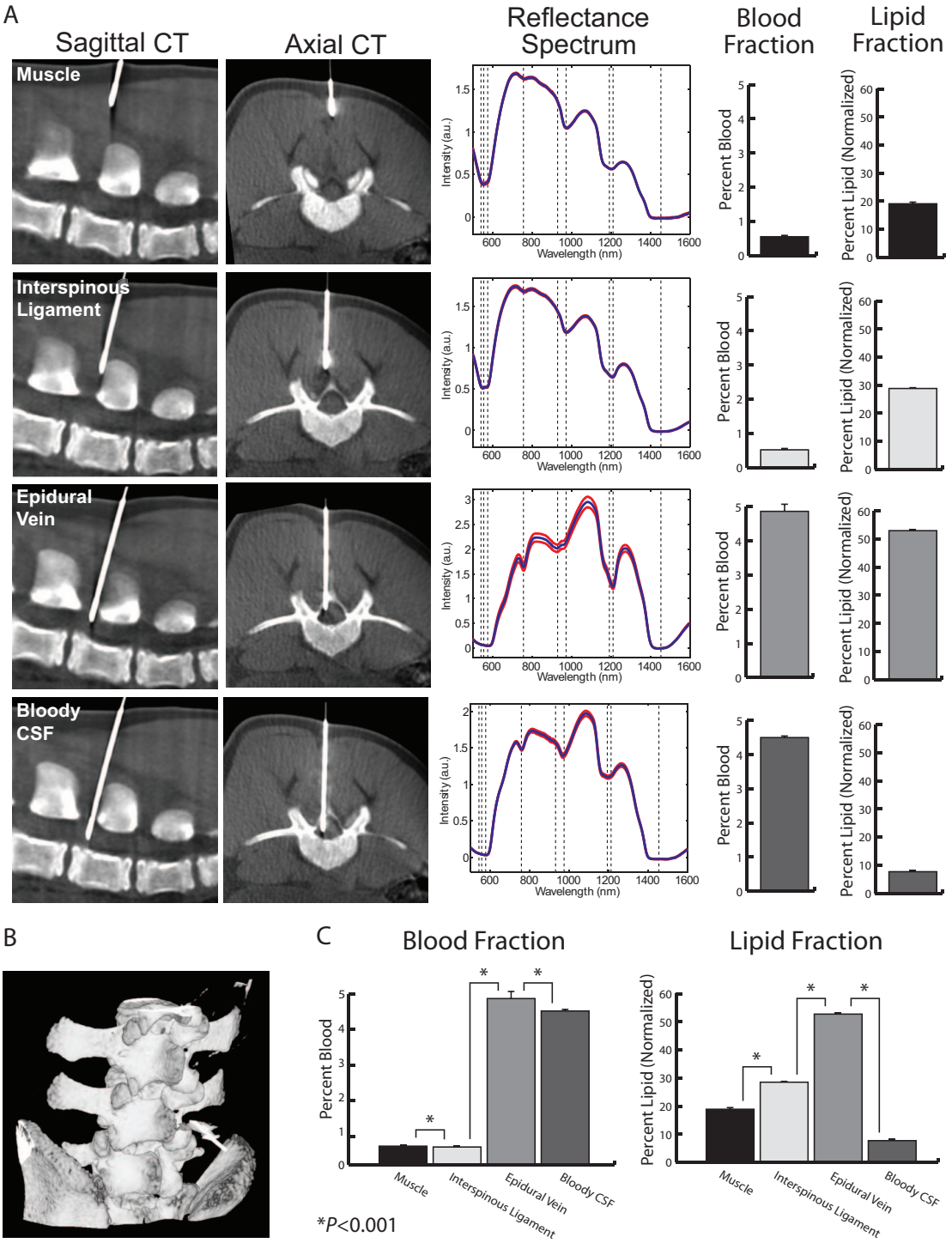

Fig. 2. Lumbar interlaminar midline approach to the epidural space (L4/5) with entry into an epidural vein. (*A*) Sagittal and axial cross-sections extracted from the XperCT image volumes (*left*) for four needle tip locations: muscle, interspinous ligament, epidural vein, and bloody cerebrospinal fluid (CSF). The corresponding optical spectra and the blood and lipid fractions are shown on the *right*. The optical spectra indicate the intensity of light received by the optical spinal needle (linear units) as a function of the wavelength. Mean spectral values (*blue*) and SD relative to the mean (*red*) are displayed as a function of wavelength. Specific wavelengths corresponding to selected absorption peaks are indicated with *dashed lines*. Oxyhemoglobin: 542 and 576 nm; deoxyhemoglobin: 557 and 757 nm; lipids: 930 and 1,210 nm; water: 976, 1197, and 1,455 nm. (*B*) Surface rendering of the XperCT volume indicating the needle trajectory relative to the spine. (*C*) Blood and lipid fractions concatenated to indicate their variation as the needle tip progressed ventrally. An *asterisk* indicates a transition for which the corresponding parameter change within this insertion was statistically significant at the level of $P < 0.001$ using two-tailed *t* tests for paired samples ($P < 0.0167$ considered significant after Bonferroni correction for multiple comparisons). CT = computed tomography.

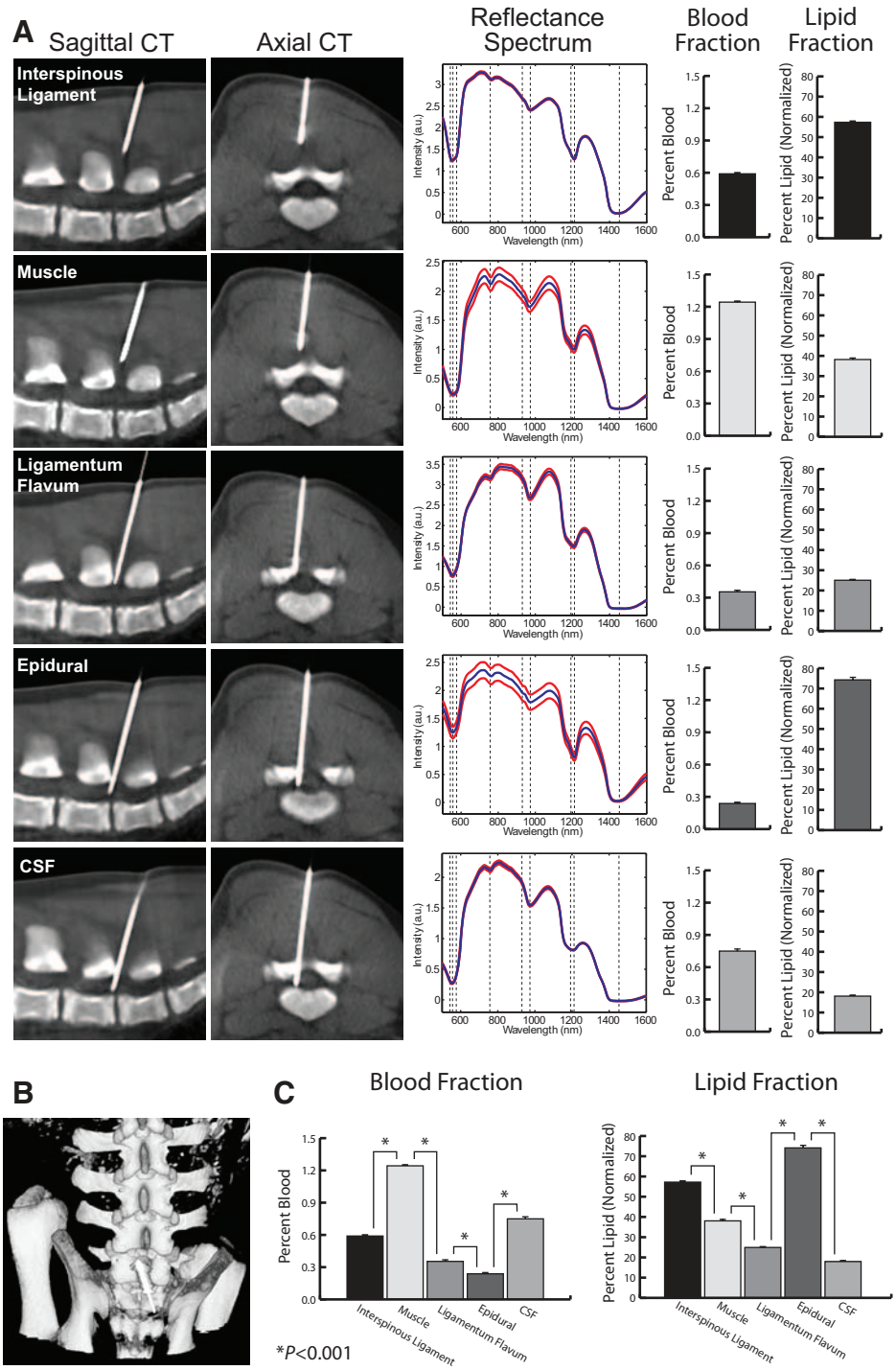

Fig. 3. Lumbar interlaminar midline approach to the epidural space (L5/6) with lateral deviation from midline. (*A*) Sagittal and axial cross-sections extracted from the XperCT image volumes (*left*) for five needle tip locations: interspinous ligament, muscle, ligamentum flavum, epidural space, and cerebrospinal fluid (CSF). The corresponding optical spectra and the blood and lipid fractions are shown on the *right*. The optical spectra indicate the intensity of light received by the optical spinal needle (linear units) as a function of the wavelength. Mean spectral values (*blue*) and SD relative to the mean (*red*) are displayed as a function of wavelength. Specific wavelengths corresponding to selected absorption peaks are indicated with *dashed lines*. Oxyhemoglobin: 542 and 576 nm; deoxyhemoglobin: 557 and 757 nm; lipids: 930 and 1,210 nm; water: 976,1197, and 1,455 nm. (*B*) Surface rendering of the XperCT volume indicating the needle trajectory relative to the spine. (*C*) Blood and lipid fractions concatenated to indicate their variation as the needle tip progressed ventrally. An *asterisk* indicates a transition for which the corresponding parameter change within this insertion was statistically significant at the level of $P < 0.001$ using two-tailed *t* tests for paired samples ($P < 0.0125$ considered significant after Bonferroni correction for multiple comparisons). CT = computed tomography.

two parameters (25.1 ± 0.4% and 0.36 ± 0.02%, respectively). The transition of the needle tip from the epidural space into the intrathecal space was associated with a decrease in the lipid fraction and an increase in the blood fraction (fig. 3). With the needle tip in the intrathecal space, removal of the stylet revealed backflow of clear CSF.

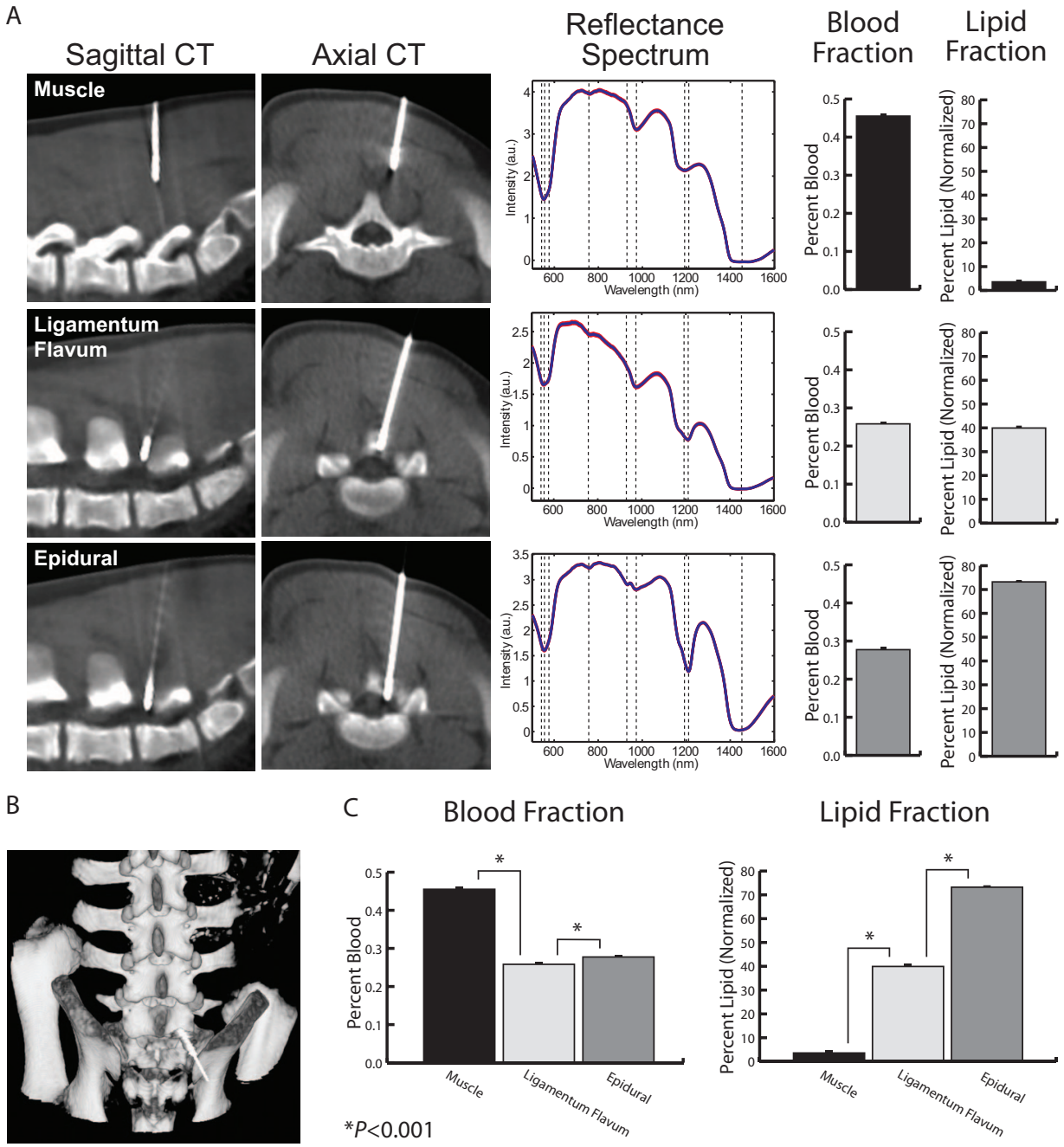

Fig. 4. Lumbar interlaminar paramedian approach to the epidural space (L5/6). (*A*) Sagittal and axial cross-sections extracted from the XperCT image volumes (*left*) for three needle tip locations: muscle, ligamentum flavum, and epidural space. The corresponding optical spectra and the blood and lipid fractions are shown on the *right*. The optical spectra indicate the intensity of light received by the optical spinal needle (linear units) as a function of the wavelength. Mean spectral values (*blue*) and SD relative to the mean (*red*) are displayed as a function of wavelength. Specific wavelengths corresponding to selected absorption peaks are indicated with *dashed lines*. Oxyhemoglobin: 542 and 576 nm; deoxyhemoglobin: 557 and 757 nm; lipids: 930 and 1210 nm; water: 976, 1197, and 1455 nm. (*B*) Surface rendering of the XperCT volume indicating the needle trajectory relative to the spine. (*C*) Blood and lipid fractions concatenated to indicate their variation as the needle tip progressed ventrally. An *asterisk* indicates a transition for which the corresponding parameter change within this insertion was statistically significant at the level of $P < 0.001$ using two-tailed *t* tests for paired samples ($P < 0.025$ considered significant after Bonferroni correction for multiple comparisons). CT = computed tomography.

Figure 4 illustrates a paramedian approach to the lumbar epidural space, traversing from the paraspinous musculature, through the ligamentum flavum and in the epidural space near midline. Again, an increase in lipid fraction was observed with the transition of the needle tip from skeletal muscle to the epidural space (3.6 ± 0.2% to 73.2 ± 0.5%), and an intermediate value (38.9 ± 0.3%) was once again observed with the needle tip at the ligamentum flavum. As with the third insertion, a decrease in the blood fraction was also observed with the transition from skeletal muscle to ligamentum flavum in the fourth insertion; in contrast, the transition from ligamentum flavum to the epidural space transition was associated with a slight increase in the blood fraction.

Figure 5 illustrates midline needle insertion at the thoracic level. Variations in the lipid fraction were similar to those in the first and second insertions (lumbar midline), with increases observed as the needle tip progressed from skeletal muscle (32.3 ± 0.2%) to the epidural space (69.4 ± 0.3%) *via* the interspinous ligament (42.4 ± 0.3%). Interestingly, the blood fraction was high when the needle tip was directly within the spinal cord, but backflow of blood was not observed; at that location, the lipid fraction was lower than that when the needle tip was in the epidural space.

Across all epidural insertions, the mean lipid fractions obtained from skeletal muscle were 1.9- to 20-fold higher than those obtained from the epidural space. Transitions of the needle tip from adjacent ligamentous tissues (the interspinous ligament and the ligamentum flavum) to the epidural space were also associated with increases in the mean lipid fraction, which ranged from 1.6- to 3.0-fold.

The changes in both blood and lipid fractions corresponding to transitions from one tissue type to another for individual needle insertions were found to be significant in all cases ($P < 0.001$). For every transition, the pairwise comparisons that were tested for each needle insertion are shown graphically in figures 1C–5C; the differences in blood and lipid fractions are presented in table 1. The mean lipid fraction obtained with the optical needle tip in the epidural space was significantly higher than that obtained from adjacent ligamentous tissues for all five needle insertions ($P = 0.0020$). The mean lipid fraction obtained with the optical needle tip in the epidural space was also significantly higher than that in muscle for all five needle insertions ($P = 0.0013$). The corresponding differences in the mean blood fraction were not significant. Differences in the mean blood and lipid fractions obtained from all insertions are summarized in table 2.

Optically Guided Insertions

In each insertion that was guided solely with real-time interpretation of optical spectra, the interpreter identified a prominent absorption peak centered at 1,210 nm. These absorption peaks were visually consistent with those identified in spectra acquired from the epidural space during x-ray guided insertions. Examination of the XperCT images that were acquired after these prominent absorption peaks had been reported revealed that the needle tip had reached the epidural space at the end of each of the five consecutive insertions.

Discussion

The traditional LOR technique depends on unreliable and somewhat subjective measures of the mechanical resistance to injection of air or saline. In contrast, spectroscopic detection of the epidural space employs quantitative and reproducible parameters. The prominent lipid absorption peaks that were observed in spectra acquired from the epidural space are consistent with cryomicrotome studies, which found a predominance of homogeneous fat in the posterior epidural compartment.[20] This histologic correlate could prove to be advantageous in terms of interpreting the optical spectra. With parameters that are based on reflectance at visible wavelengths, such as those developed in a previous study,[10] histologic correlates remain to be determined; furthermore, one can expect that minor bleeding events could have a significant influence on their values. Optical identification of the epidural space with the lipid parameter may have limitations in certain clinical contexts, however, such as access to the epidural space in the cervical spine where there is a relative paucity of epidural fat[21] or with certain pathologic conditions such as spinal stenosis that are frequently accompanied by local reductions in the amount of epidural fat. The relatively small distance in front of the needle sampled for the spectral data (estimated to be approximately 1.2 mm) may well allow use, however, even when the dimensions of the epidural space are limited.

In one of the five insertions, epidural access was associated with a large increase in the blood fraction that coincided with venous backflow. That coincidence gives confidence that the optical spinal needle could provide a means for early detection of intravascular needle position, before local anesthetic or an epidural catheter are placed. However, the lipid fraction remained high, suggesting that the volume of tissue sampled at this intravenous location included both the blood around the needle tip and some of the adjacent epidural fat. More detailed studies are required to determine the distance from the bevel surface at which veins and arteries can be detected with optical spectroscopy. It is possible that perivascular needle positioning can be detected even before the vessel is entered, based on the spectral characteristics of the exterior wall of the vessel. Given the differences in the wavelength dependence of light absorption by oxygenated and deoxygenated forms of hemoglobin, refinements of the spectral processing algorithm should allow for the hemoglobin oxygenation saturation at the needle tip to be quantified. Accurate hemoglobin oxygenation saturation measurements would allow for differentiation of arterial and venous structures.

There were significant variations in both blood and lipid fractions when the needle tip was within the CSF, suggesting that the position of the needle tip relative to the thecal sac or neural elements may alter the spectral characteristics. However, transitions from the epidural space to the intrathecal space were consistently associated with large reductions of

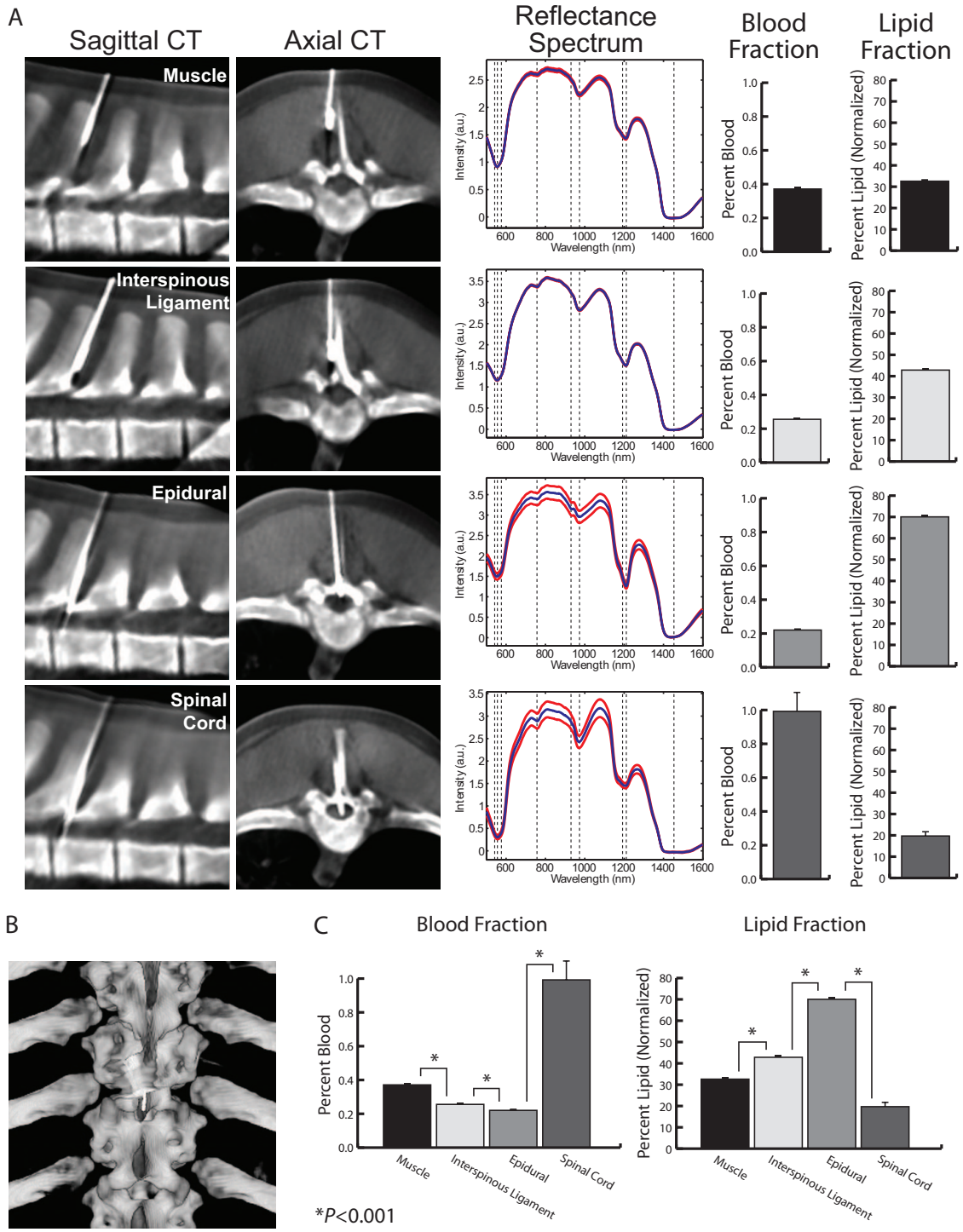

Fig. 5. Midthoracic interlaminar midline approach to the epidural space. (*A*) Sagittal and axial cross-sections extracted from the XperCT image volumes (*left*) for four needle tip locations: muscle, interspinous ligament, epidural space, and spinal cord. The corresponding optical spectra and the blood and lipid fractions are shown on the *right*. The optical spectra indicate the intensity of light received by the optical spinal needle (linear units) as a function of the wavelength. Mean spectral values (*blue*) and SD relative to the mean (*red*) are displayed as a function of wavelength. Specific wavelengths corresponding to selected absorption peaks are indicated with *dashed lines*. Oxyhemoglobin: 542 and 576 nm; deoxyhemoglobin: 557 and 757 nm; lipids: 930 and 1,210 nm; water: 976, 1197, and 1455 nm. (*B*) Surface rendering of the XperCT volume indicating the needle trajectory relative to the spine. (*C*) Blood and lipid fractions concatenated to indicate their variation as the needle tip progressed ventrally. An *asterisk* indicates a transition for which the corresponding parameter change within this insertion was statistically significant at the level of $P < 0.001$ using two-tailed *t* tests for paired samples ($P < 0.0167$ considered significant after Bonferroni correction for multiple comparisons). CT = computed tomography.

Table 1. Changes in Blood and Lipid Fractions during Individual Tissue Transitions

	Δ Blood Fraction	Δ Lipid Fraction
Insertion 1: Midline approach		
Muscle to interspinous lig.	−1.287 ± 0.012	18.028 ± 0.442
Interspinous lig. to epidural space	−0.587 ± 0.006	24.309 ± 0.422
Epidural space to CSF	0.022 ± 0.007	−36.236 ± 0.644
CSF to intervertebral disc	−0.014 ± 0.009	−9.475 ± 0.469
Insertion 2: Midline approach, entry in to epidural vein		
Muscle to interspinous lig.	−0.029 ± 0.015	9.576 ± 0.577
Interspinous lig. to epidural vein	4.259 ± 0.206	24.542 ± 0.357
Epidural vein to bloody CSF	−0.374 ± 0.215	−45.490 ± 0.394
Insertion 3: Midline approach, lateral deviation		
Interspinous lig. to muscle	0.659 ± 0.012	−19.169 ± 0.651
Muscle to lig. flavum	−0.898 ± 0.015	−13.156 ± 0.615
Lig. flavum to epidural space	−0.117 ± 0.009	49.260 ± 1.016
Epidural space to CSF	0.516 ± 0.014	−56.234 ± 1.656
Insertion 4: Paramedian approach		
Muscle to lig. flavum	−0.197 ± 0.007	35.342 ± 0.374
Lig. flavum to epidural space	0.019 ± 0.009	34.275 ± 0.687
Insertion 5: Thoracic level, paramedian approach		
Muscle to interspinous lig.	−0.115 ± 0.003	10.159 ± 0.362
Interspinous lig. to epidural space	−0.035 ± 0.004	26.934 ± 0.464
Epidural space to spinal cord	0.772 ± 0.114	−49.868 ± 2.159

Data are expressed in mean ± SD, with n = 20 for each needle tip position.
CSF = cerebrospinal fluid; lig. = ligament.

the lipid fraction. In all three insertions in which this transition was tested, the mean reductions ranged from 4.1- to 6.9-fold. This suggests that optical spectroscopy allows for ready detection of entry into the thecal sac, potentially obviating the need to use a test dose of local anesthetic as the only reliable test to rule out intrathecal placement. However, the measurement geometry is important for interpreting the spectroscopic information. Even when the opening of the needle cannula is completely within the intrathecal space, a part of the long bevel surface and the distal end of at least one optical fiber may be in adjacent tissues. Optical absorption in these adjacent tissues could produce a large lipid fraction, falsely leading the operator to conclude that the entire needle is within the epidural space. Another confounding factor is that the scattering of light in clear CSF is much lower than in tissues, so that measured light probably derived in part from tissues enclosing the intrathecal space.

Spectroscopic detection of spinal cord penetration could be valuable for preventing rare but potentially devastating injections within the spinal cord. The high blood fraction and the prominent deoxyhemoglobin absorption peaks observed after the needle tip penetrated the spinal cord (fig. 5) may have resulted from bleeding within the spinal cord after needle penetration. Further study is needed to determine to what extent optical spectroscopy can detect intracord needle tip placement.

Penetration into the intervertebral disc (fig. 1) is not typically a concern with fluoroscopically guided epidural steroid injections performed in clinical practice because this structure is so far anterior. The present study demonstrated a distinctive spectral pattern within the disc, another example of the potential for tissue differentiation with optical spectroscopy: both the blood and lipid fractions changed significantly during the transition of the needle tip from the epidural space to the intervertebral disc.

The optical signals acquired from a particular location in tissue probably depend to some extent on the tissues encountered at previous times during the insertion. For instance, as the needle tip progressed through tissues, a small volume of blood could have remained close to the bevel surface and altered the spectroscopic signals; the extent to which this effect manifested is unclear. Blood could also have diffused into the intrathecal space together with the needle tip, particularly if an epidural vein was punctured. This situation

Table 2. Differences in Mean Blood and Lipid Fractions Obtained from all Insertions

	Mean Difference in Blood Fraction	*P* Value	Mean Difference in Lipid Fraction	*P* Value
Muscle *vs.* epidural space	0.203 ± 2.360	0.844	43.854 ± 14.719	0.0013
Lig. tissue *vs.* epidural space	0.708 ± 1.999	0.489	31.864 ± 10.529	0.0020

Data are expressed in mean ± SD, with n = *5* for each comparison.
P = values of two-tailed *t* test for paired samples (unequal variances).
Lig. tissue = ligamentous tissue, interspinous ligament, or ligamentum flavum, depending on the insertion.

was likely encountered in the second insertion; it is consistent with the increased blood fraction observed when the needle tip was in the intrathecal space.

Several confounding factors can decrease the accuracy of the blood and lipid fraction estimates and their interpretation. For the blood fraction, they include the presence of additional tissue chromophores, such as myoglobin in muscle and carotenes in epidural fat.[22] The total hemoglobin content of blood in swine is broadly similar to that in humans, but variations as a function of age and sex are known to occur in both species[23,24]; as such, a degree of caution is warranted when interpreting relating blood fraction to whole blood. For the lipid fraction, confounding factors may include the presence of chromophores such as collagen.[25] Variations in optical scattering, such as those induced by tissue compression[26] during needle insertions, may affect the average distance traveled by light in tissue and thereby affect the volume of tissue from which a spectrum derives.

Variations in the angle of the needle bevel with respect to tissue layer interfaces probably contributed significantly to the intrainsertion differences of the lipid and blood fractions. This effect was identified in the study by Ting *et al.*[10] For instance, in cases where the needle tip was within muscle, spectroscopic signals could have been influenced by the presence of adjacent fascia, depending on the angle of the bevel. Likewise, in cases where the needle tip was in close proximity to the interspinous ligament, spectroscopic signals could have been influenced by the presence of adjacent adipose and skeletal muscle tissues. The pressure imparted by the needle on tissues may have altered the geometric arrangement of the tissue layer interfaces and the angle of the needle bevel. In cases where the needle tip was in contact with the ligamentum flavum and little pressure was applied, one could expect spectroscopic signals to derive primarily from skeletal muscle. When more pressure was applied, the ligamentum flavum surface may have been deformed, so that more light was primarily directed ventrally toward the epidural fat; one could expect a higher lipid fraction in this case.

Lateral deviation of the needle tip from the interspinous ligament to adjacent skeletal muscle during midline insertions occurs relatively frequently in clinical practice. This deviation can result in false LOR and failed epidural anesthesia when decreased resistance to injection of air or saline occurs as the needle tip enters muscle. Spectroscopic signals could differentiate between true LOR in the epidural space and false LOR in skeletal muscle. In this study, the latter event was associated with a lower lipid fraction and a higher blood fraction; the former, with a higher lipid fraction and frequently with a lower blood fraction.

Relative changes in the blood and lipid fractions that occur in a particular insertion may provide more robust indications of epidural space access than absolute values. For instance, the lipid fraction obtained from the epidural space in the first insertion was only 1.2-fold higher than that obtained from ligamentum flavum in the fourth insertion. However, in both of those insertions, epidural space access was associated with an increase in lipid fraction of at least 1.9-fold relative to those obtained from adjacent tissues. Relative changes in the blood and lipid fractions are not likely to be uniquely associated with specific tissue layer transitions, as hemoglobin and lipid concentrations vary widely in tissues encountered during epidural injections. Because the optical spectra are acquired from tissues that are very close to the bevel surface, we expect that correct interpretation of spectroscopic information may ultimately depend on image guidance to indicate the locations of anatomic landmarks relative to the needle tip (*e.g.*, fluoroscopy or ultrasound).

The encouraging results obtained in this *in vivo* swine study set the stage for larger-scale studies. If similar spectroscopic changes associated with epidural access are observed consistently in humans, they could indicate the correct endpoints of epidural injections in real time. In this way, the optical spinal needle has the potential to increase the efficacy of epidural injections and reduce the incidence of complications, such as intravascular injection, dural puncture, intrathecal injection, and spinal cord damage. The optical spinal needle would therefore be complementary to fluoroscopic imaging, providing soft-tissue contrast for tissues that has never before been available.

The authors thank Pellina Janson, Technician, Karolinska Experimental and Research Imaging Center, Karolinska University Hospital, Stockholm, Sweden.

References

1. Heran MK, Smith AD, Legiehn GM: Spinal injection procedures: A review of concepts, controversies, and complications. Radiol Clin North Am 2008; 46:487–514
2. Stojanovic MP, Vu TN, Caneris O, Slezak J, Cohen SP, Sang CN: The role of fluoroscopy in cervical epidural steroid injections: An analysis of contrast dispersal patterns. Spine 2002; 27:509–14
3. Hogan QH: Epidural anatomy examined by cryomicrotome section. Influence of age, vertebral level, and disease. Reg Anesth 1996; 21:395–406
4. Abram SE: Intrathecal steroid injection for postherpetic neuralgia: What are the risks? Reg Anesth Pain Med 1999; 24:283–5
5. Ho KY: Vascular uptake of contrast despite negative aspiration in interlaminar cervical epidural injection. Pain Physician 2006; 9:267–8
6. Hodges SD, Castleberg RL, Miller T, Ward R, Thornburg C: Cervical epidural steroid injection with intrinsic spinal cord damage. Two case reports. Spine 1998; 23:2137–42
7. Tripathi M, Nath SS, Gupta RK: Paraplegia after intracord injection during attempted epidural steroid injection in an awake-patient. Anesth Analg 2005; 101:1209–11
8. Rathmell JP: Atlas of Image-Guided Intervention in Regional Anesthesia and Pain Medicine. Philadelphia, Lippincott Williams & Wilkins, 2005
9. Shetty SK, Nelson EN, Lawrimore TM, Palmer WE: Use of gadolinium chelate to confirm epidural needle placement in patients with an iodinated contrast reaction. Skeletal Radiol 2007; 36:301–7
10. Ting CK, Tsou MY, Chen PT, Chang KY, Mandell MS, Chan KH, Chang Y: A new technique to assist epidural needle placement: Fiberoptic-guided insertion using two wavelengths. ANESTHESIOLOGY 2010; 112:1128–35
11. Racadio JM, Babic D, Homan R, Rampton JW, Patel MN,

Racadio JM, Johnson ND: Live 3D guidance in the interventional radiology suite. AJR Am J Roentgenol 2007; 189: W357–64

12. Söderman M, Babic D, Holmin S, Andersson T: Brain imaging with a flat detector C-arm: Technique and clinical interest of XperCT. Neuroradiology 2008; 50:863–8
13. Sack WO: Essentials of Pig Anatomy. Ithaca, Veterinary Textbooks, New York, 1982, pp 18
14. Zonios G, Perelman LT, Backman V, Manoharan R, Fitzmaurice M, Van Dam J, Feld MS: Diffuse reflectance spectroscopy of human adenomatous colon polyps *in vivo*. Appl Opt 1999; 38:6628–37
15. Nachabé R, Hendriks BH, Desjardins AE, van der Voort M, van der Mark MB, Sterenborg HJ: Estimation of lipid and water concentrations in scattering media with diffuse optical spectroscopy from 900 to 1,600 nm. J Biomed Opt 2010; 15:037015
16. Schenkman KA, Marble DR, Feigl EO, Burns DH: Near-infrared spectroscopic measurement of myoglobin oxygen saturation in the presence of hemoglobin using partial least-squares analysis. Appl Spectrosc 1999; 53:325–31
17. Conway JM, Norris KH, Bodwell CE: A new approach for the estimation of body composition: Infrared interactance. Am J Clin Nutr 1984; 40:1123–30
18. Anderson RR, Farinelli W, Laubach H, Manstein D, Yaroslavsky AN, Gubeli J 3rd, Jordan K, Neil GR, Shinn M, Chandler W, Williams GP, Benson SV, Douglas DR, Dylla HF: Selective photothermolysis of lipid-rich tissues: A free electron laser study. Lasers Surg Med 2006; 38:913–9
19. Kou L, Labrie D, Chylek P: Refractive indices of water and ice in the 0.65- to 2.5-μm spectral range. Appl Opt 1993; 32:3531–40
20. Hogan QH: Lumbar epidural anatomy. A new look by cryomicrotome section. ANESTHESIOLOGY 1991; 75:767–75
21. Chin CT: Spine imaging. Semin Neurol 2002; 22:205–20
22. Reina MA, Franco CD, López A, Dé Andrés JA, van Zundert A: Clinical implications of epidural fat in the spinal canal. A scanning electron microscopic study. Acta Anaesthesiol Belg 2009; 60:7–17
23. Miller ER, Ullrey DE, Ackermann I, Schmidt DA, Luecke RW, Hoefer JA: Swine hematology from birth to maturity. II. Erythrocyte population, size and hemoglobin concentration. J Anim Sci 1961; 20:890–7
24. Hawkins WW, Speck E, Leonard VG: Variation of the hemoglobin level with age and sex. Blood 1954; 9:999–1007
25. Caplan JD, Waxman S, Nesto RW, Muller JE: Near-infrared spectroscopy for the detection of vulnerable coronary artery plaques. J Am Coll Cardiol 2006; 47:C92–6
26. Chan EK, Sorg B, Protsenko D, O'Neil M, Motamedi M, Welch AJ: Effects of compression on soft tissue optical properties. IEEE J Sel Top Quantum Electron 1996; 2:943–50